Electronic Supplementary Material (ESI) for Food & Function.

Supplemental Materials for

The dairy-derived peptide Miltin exerts anti-obesity effects by increasing adipocyte thermogenesis

Hong Zhong *et al.*

Corresponding authors: Chenbo Ji, chenboji@njmu.edu.cn; Xianwei Cui, xwcui@njmu.edu.cn; Xia Chi, chixia2001@njmu.edu.cn.

Supplementary Materials and Methods

Adipocytes culture and differentiation

Primary human brown pre-adipocytes were separated and differentiated. Cells were cultured in PAM medium (Sciencell, CA, USA) containing 5% FBS, 1% preadipocyte growth supplement and 1% penicillin/streptomycin until confluence. Differentiation was induced by DMEM/F12 medium containing 100 nM insulin, 0.5 mM 3-isobutyl-1-methylxanthine, 17 μM Pantothenate, 1 μM dexamethasone, 1 μM rosiglitazone, 33 μM d-Biotin, 10 μg/ml apo-transferrin and 1 nM triiodothyronine. After 4 day of induction, cells were moved to maintenance DMEM/F12 medium with 100 nM insulin and 1 nM triiodothyronine for 2 day. Human white pre-adipocytes were obtained from ScienCell Research Laboratories (San Diego, CA, USA) and maintained in PAM medium as brown adipocytes. Adipogenesis was initiated by DMEM/F12 medium with 0.5 mM 3-isobutyl-1-methylxanthine, 500 nM insulin, 1 μM dexamethasone and 1 μM rosiglitazone for 4 days. Then, the medium was replaced by one containing 500 nM insulin and replenished every 2 days until fully differentiated.

Cell viability

The cell viability assay was performed using Cell Counting Kit-8 (CCK-8, Dojindo Laboratories, Kumamoto, Japan) to exclude the cytotoxicity of Miltin. Briefly, brown and white adipocytes were seeded in 96-well plates and incubated with 10 or 50 μM

Miltin for 0-72 h. The absorbance at 450 nm was determined after introducing with CCK-8 solution for 3 h at 37 °C.

Metabolic phenotyping

For GTT, mice fasted overnight and were i.p. injected with 2 g/kg D-glucose. The dose of glucose injection for GTT assays performed in HFD mice was decreased to 1 g/kg per mouse. For ITT, mice were i.p. injected with 0.75 units/kg insulin after 6 h fasting. The dose of insulin used for ITT assays performed in HFD mice was increased to 1 unit/kg per mouse. Glucose levels were measured at 0, 30, 60, 90 and 120 min after injection using a glucometer (Roche, Germany).

Molecular studies

According to the manufacturer's instruments, the total RNA of cells or tissues was isolated with TRIzol (Invitrogen, USA). The concentration and purity of RNA were assessed with BioDrop Duo, and 500 ng of RNA from each sample were reverse transcribed into first strand cDNA using PrimeScriptTM RT master mix kit (Takara, Shiga, Japan). Gene expression levels were quantified with the ViiA 7 Real-Time PCR system (Thermo Fisher Scientific) using the SYBR Green method. The expression level of target mRNA was normalized to PPIA (peptidylprolyl isomerase A) and analyzed by the comparative $2^{-\triangle\triangle Ct}$ method. Primer sequences are shown in Supplemental table S1.

For Western blot analysis, homogenized tissues and cells were lysed in RIPA buffer (Beyotime, China) and quantified by BCA Protein Assay Kit (Thermo Fisher Scientific). Protein lysates were separated by SDS-PAGE and electroblotted to the PVDF membrane (Millipore). The membranes were blocked and incubated overnight with appropriate primary antibodies, and then visualized by horseradish peroxidase-conjugated secondary antibodies. The GAPDH was used as a loading control. Fluorescent images were captured by the FluorChem M system (Proteinsimple, USA). The quantitative analysis was performed by using the NIH Image J software (version: 1.52i).

Histology analysis

The BAT and iWAT tissues were embedded in paraffin and cut into 5-μm thick sections after fixing with 4% paraformaldehyde for 24 h. For immunohistochemistry, slides were probed with primary antibodies against UCP1 (1:200; Abcam, ab10983) overnight at 4℃. The horseradish peroxidase-tagged secondary antibody was used to visualize the bonded antibody in combination with a commercially available DAB kit (Vector Laboratories). Hematoxylin was used for counterstaining. For H&E staining, standard procedures were performed on 5-μm paraffin-embedded BAT and iWAT sections. All pictures were obtained using a fluorescence microscope (Zeiss, Imager. A2, Oberkochen, Germany).

Plasma parameters

Commercial kits were used to determine the serum levels of insulin, ALT and AST (Millipore, Billerica, MA; USA). Serum triglyceride concentrations were measured using the triglyceride assay kit (Applygen Technologies Inc.).

RNA-seq

The changes in transcriptome profiling initiated by Miltin in brown adipocytes were measured by next-generation sequencing. The library was constructed from purified poly-A-containing mRNA and was sequenced on the Illumina HiSeq X-ten (Illumina, USA). Cleaned reads were mapped to the human GRCh38 reference genome with two mismatches using Hisat2 (version: 2.0.4). Stringtie (version: 1.3.0) was run to calculate Fragments Per Kilobase of transcript per Million mapped reads for further statistics. Transcripts with fold changes ≥ 2 and P value ≤ 0.05 were defined as significant. KEGG analysis was applied to identify the potential pathways of differently expressed genes.

Immunofluorescence staining

Brown and white pre-adipocytes were seeded separately in an 8-well chamber slide for 12 hours. FITC-labeled peptides were added into the chamber with a final concentration of 50 μM. After 3 h incubation, cells were washed three times with PBS to exclude the additional FITC-labeled peptides. Nuclei were counterstained with

DAPI (Thermo Fisher Scientific) in PBS for 5 min. Images were captured using a fluorescence microscope (Zeiss, Imager. A2).

Site-directed mutagenesis and recombinant protein purification

The plasmid expressing full-length human GADD45γ protein (pET-30a-GADD45γ-WT) was constructed by Merry Bio Co., Ltd. (Nanjing, China). The Gln20 to Asn (pET-30a-GADD45γ-Q20N) and Glu166 to Asp (pET-30a-GADD45γ-E166D) mutants were generated using the ThermoFisher Phusion Site-Directed Mutagenesis Kit following the suggested instructions. The mutated clones were confirmed by sequencing. To express the wild-type and mutant GADD45γ proteins, the recombinant plasmids were transformed into competent BL21 (DE3) strain. The bacteria were cultured in LB medium and protein expression was induced by isopropyl-beta-D-thiogalactopyranoside (IPTG). Cells were then lysed and spun to remove the debris. The target protein GADD45γ in the supernatant was purified with Ni-NTA His-Bind resin and analyzed by Western blotting.

Analytical method for Miltin

Commercial whole milk was purchased from supermarkets, while human milk was donated from healthy lactating mothers at the Women's Hospital of Nanjing Medical University. Ethics approval for the human milk sample collection was obtained by the Ethics Committee of Nanjing Maternity and Child Health Care Hospital (permit

number 2022LSKY-018). For peptide extraction, 150 μL of milk sample aliquots were poured into a 10-mL glass, 300 μL of 20% acetonitrile (ACN) was added, and the sample was incubated at 4°C for 30 min to completely disrupt the protein–peptide interactions. To precipitate abundant proteins such as casein and transfer protein, 1.2 mL pure ACN was added and vortexed for 20 s. The mixture was centrifuged at 3000 × g for 10 min at 4 °C and supernatant was concentrated by Speed-Vac (Taicang Hualida Laboratory Equipment Co., Ltd., Taicang, China). The dried low molecular weight fraction was redissolved in 0.1% formic acid and subsequently analyzed by liquid chromatography–tandem mass spectrometry (LC–MS/ MS).

The LC–MS/ MS analyses were carried out with a Jasper HPLC system coupled to a 4500 MD Mass Spectrometer (ABsciex, USA). Chromatographic separation was achieved using an ACUITY UPLC BEH, C18 column (2.1 × 50 mm, 1.7 μm). The mobile phase A was a mixture of 0.1% formic acid in HLPC grade water, while 0.1% formic acid in ACN was used as mobile phase B. Gradient elution was performed with a flow rate of 0.3 mL/min. The injection volume was 5 μL. The mass spectrometer was operated in the positive mode. Multiple ion transitions of m/z 437.53 → 646.323, 437.53 → 244.166 and 292.02 → 315.203, and a 3.5 min retention time were used to identify Miltin. Quantification was determined based on the peak areas using Analyst Software on the instrument. Concentrations of test

samples were interpolated from a standard curve and normalized to milk sample volume.

Supplemental Figures

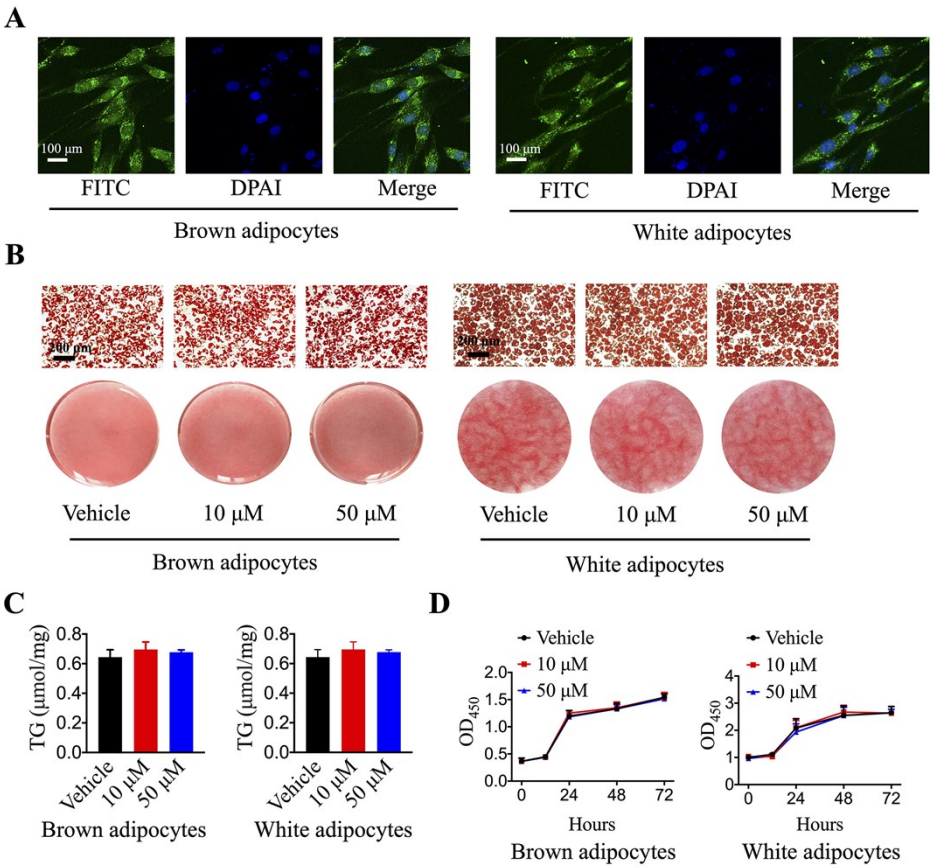

Supplemental Fig. S1 Miltin causes no change in adipogenesis of pre-adipocytes
(A) Representative images of brown and white preadipocytes treated with FITC-labeled (green) Miltin for 2 h. Nuclei were stained with DAPI (blue). Overlays of the green and blue channels are represented in the "Merge" panel. (B and C) Human brown and white preadipocytes were treated with 10 μM and 50 μM Miltin at day 0 of differentiation. Oil red O staining (B) and TG determination (C) were performed until fully differentiated. (D) Cell viability was determined using a Cell Counting Kit-8. Data are presented as mean ± SD.

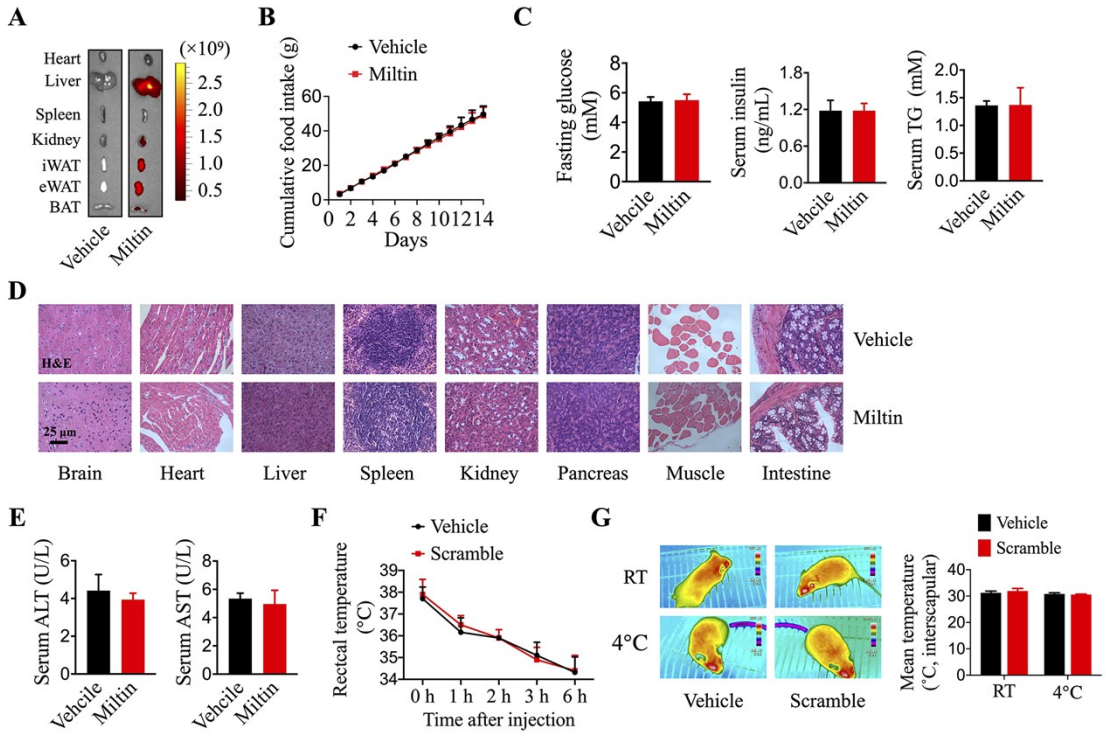

Supplemental Fig. S2 Miltin causes no significant serological and histological changes in C57BL/6J mice fed a chow diet

(A) In vitro fluorescence imaging of excised organs. Mice were i.p. injected with FITC-conjugated Miltin or vehicle, and imaging was performed at 3 h after injection. (B-D) C57BL/6J mice fed a chow diet were i.p. injected with 10 mg/kg Miltin or vehicle for 2 weeks (n=5/group). (B) Cumulative food intake of mice following the 2 weeks injection. (C) Serum levels of glucose, insulin and TG. (D) Representative histology data (H&E) of tissues excised from mice injected with Miltin or vehicle. Magnification: 200 x. (E) Serum levels of ALT and AST. (F and G) The scrambled peptide or vehicle was injected into 6-8 weeks old C57BL/6J mice (n=5/group) daily for 2 weeks on a chow diet. Core body temperature (F) and skin temperature (G) were evaluated either at ambient room temperature or exposure to 4˚C. Data are presented as mean ± SD.

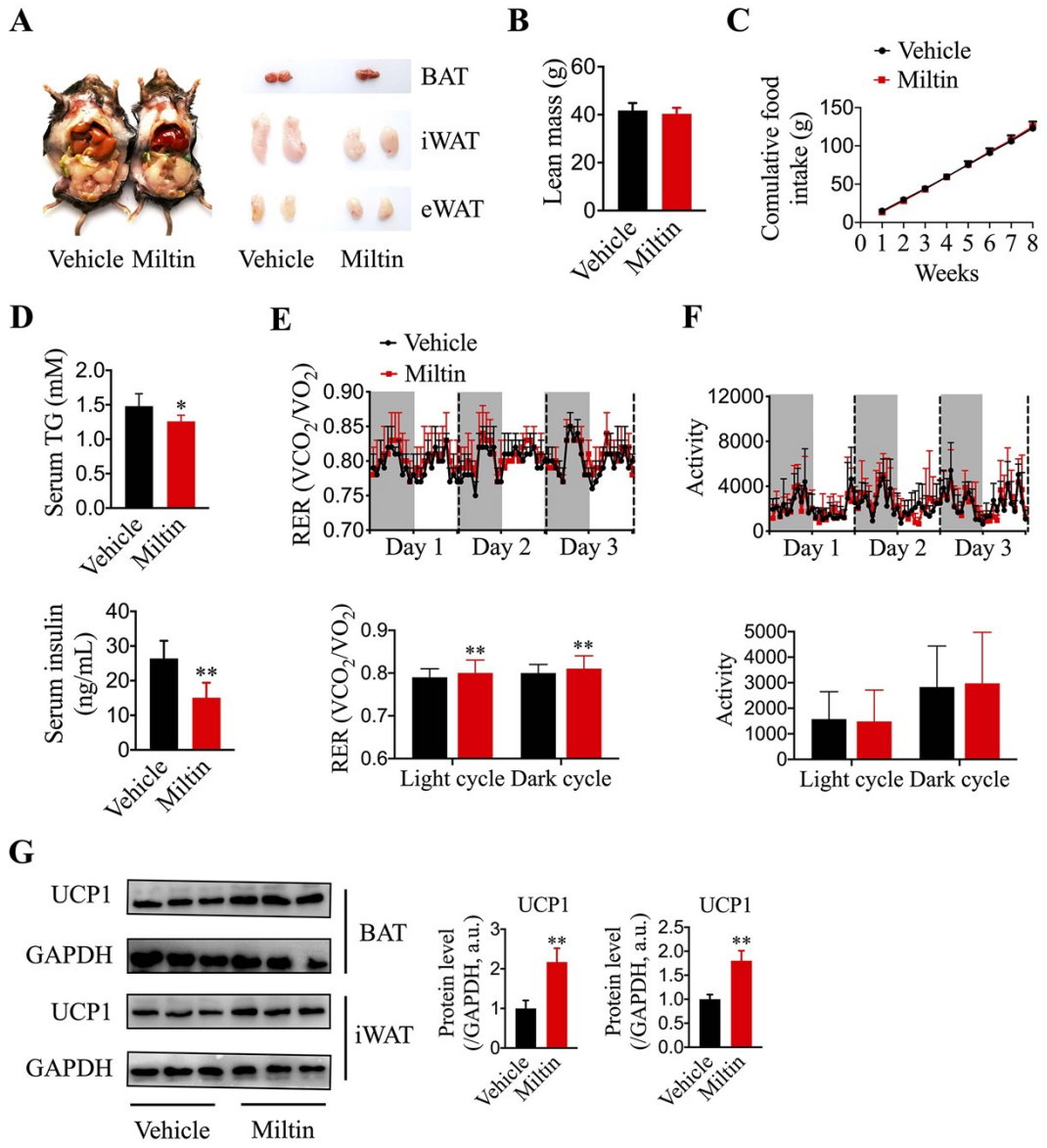

Supplemental Fig. S3 Miltin improves obesity signature in DIO mice by increasing energy expenditure

(A-H) Mice fed an HFD for 6 months were injected with Miltin or vehicle for another 8 weeks at room temperature. (A) Representative pictures of mice after Miltin treatment. (B and C) Lean mass by NMR scans (B) and cumulative food intake (C) of mice treated with Miltin as compared with vehicle control. (D) Serum TG and insulin concentrations. (E and F) Respiratory exchange ratios (RERs) and locomotor activity were measured in metabolic cages for the Miltin-treated group and vehicle control (top, n=6/group). The gray part indicates the dark phase. The bottom bar graphs represent the average for each group. (G) Immunoblots of UCP1 (left) and densitometric quantification normalized to loading control GAPDH (right). Data are presented as mean ± SD. $^{*}P < 0.05$ and $^{**}P < 0.01$ versus Vehicle, two-tailed unpaired Student's *t* tests (D to G).

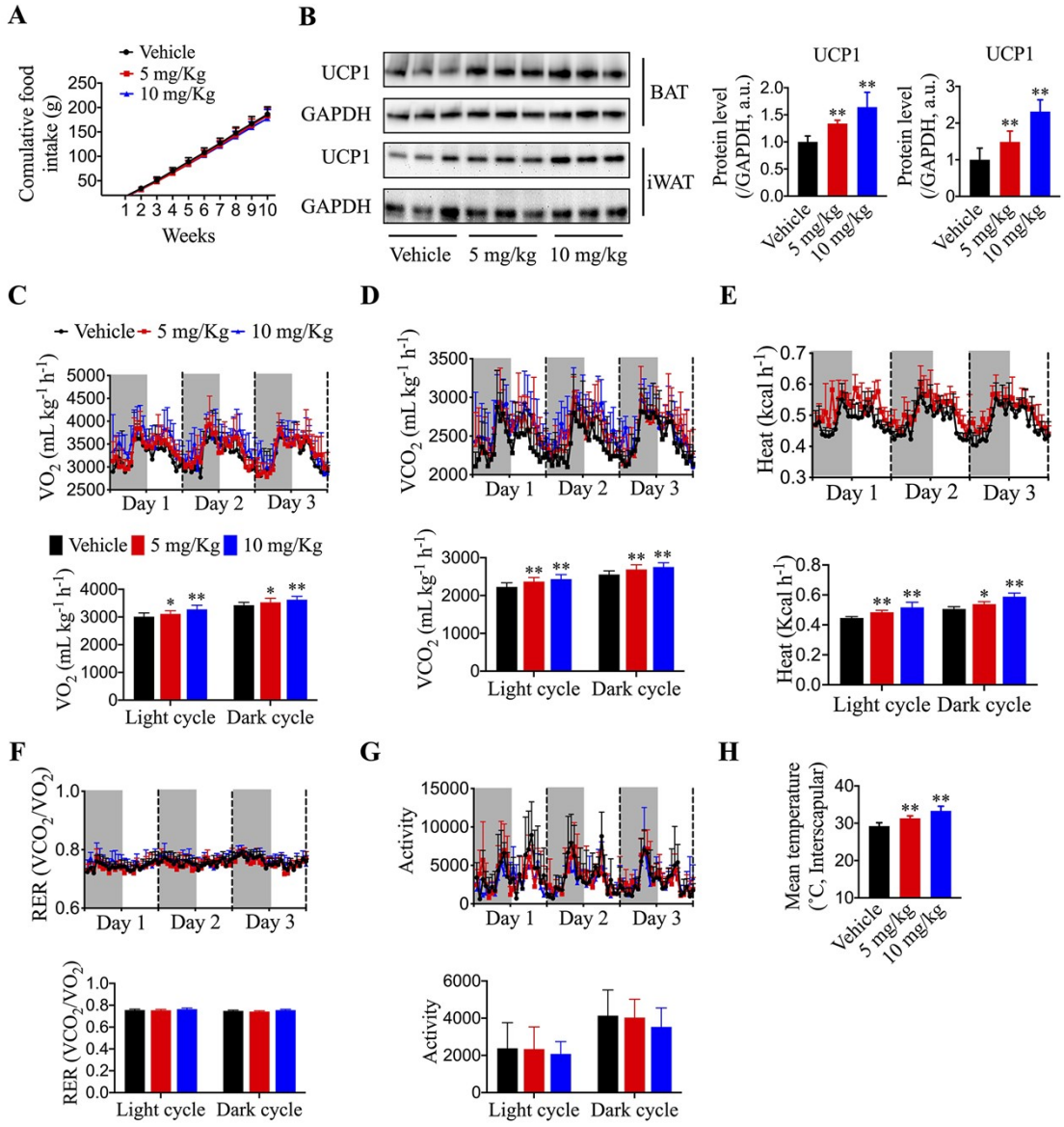

Supplemental Fig. S4 Miltin increases energy expenditure and confers resistance to diet-induced obesity

(A) Cumulative food intake. (B) Expression of UCP1 protein levels was detected in BAT and iWAT deposits. (C to G) O_2 consumption (C), CO_2 production (D), heat generation (E), RER (F) and locomotory activity (G) were measured in metabolic cages to evaluate the energy expenditure changes after Miltin treatment (n=4/group). The gray part indicates the dark phase. The bottom bar graphs represent the average for each group. (H) Skin temperature quantification of infrared images. Data are presented as mean ± SD. $^{*}P < 0.05$ and $^{**}P < 0.01$ versus Vehicle, two-tailed unpaired Student's *t* tests (B-H).

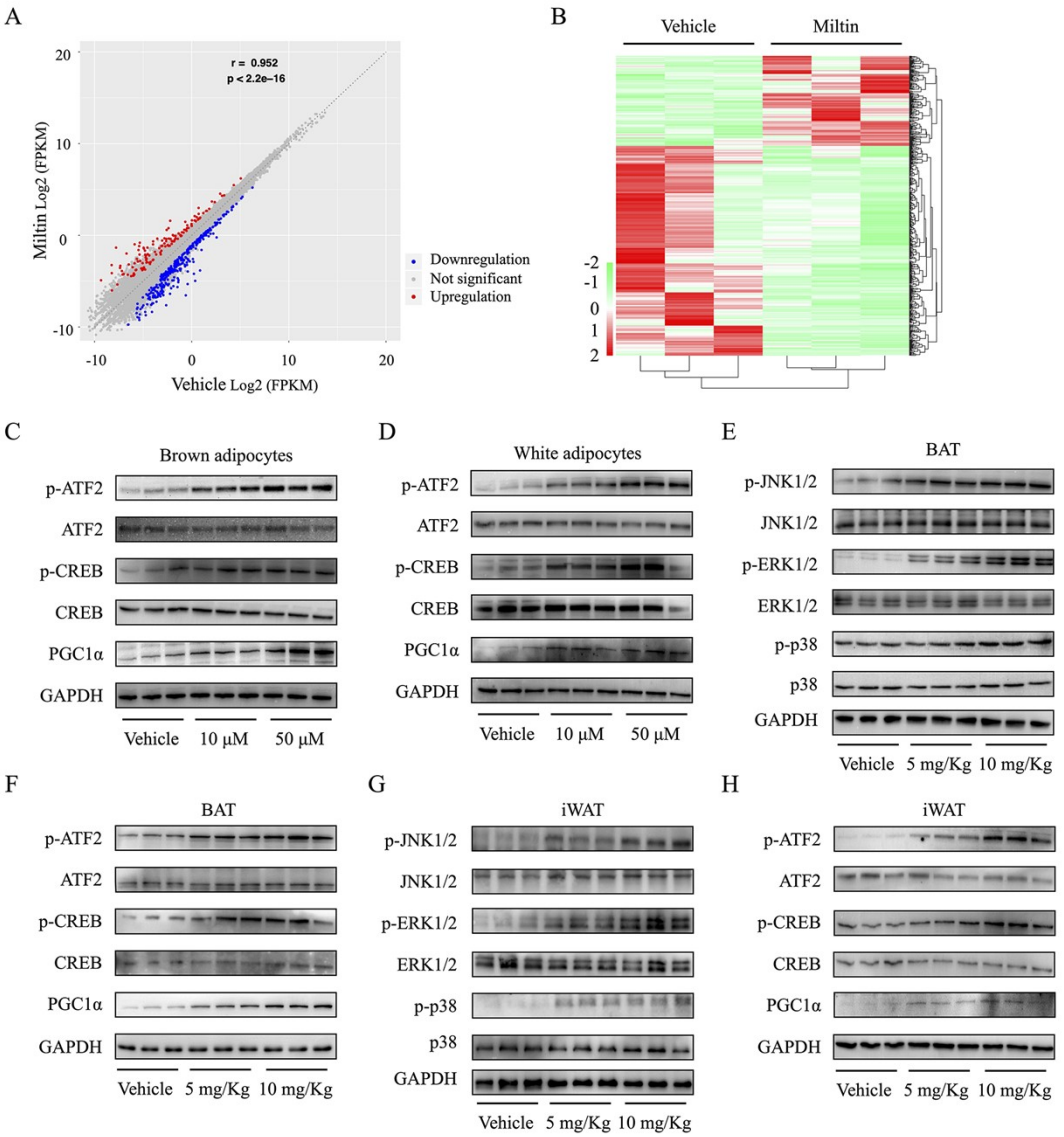

Supplemental Fig. S5 MAPK signaling pathway is involved in the Miltin-mediated thermogenesis of adipocytes

Brown adipocyte samples were collected after 3 h of Miltin stimulation and gene expression changes were profiled by next-generation sequencing (RNA-Seq). (A) The scatter plot in the log2 scale indicates the fold changes of gene expression in Miltin-treated brown adipocytes compared with vehicle control. (B) Hierarchical clustering showing up and downregulated genes induced by Miltin treatment. (C and D) Immunoblots indicate the phosphorylated and total protein levels of ATF2 and CREB and the PGC1α protein level in mature brown and white adipocytes. (E-H) Immunoblots for the phosphorylation of JNK, ERK1/2, p38, ATF2 and CREB as well as the PGC1α protein level in BAT and iWAT from C57BL6J mice fed a chow diet administrated with Miltin or vehicle for 2 weeks.

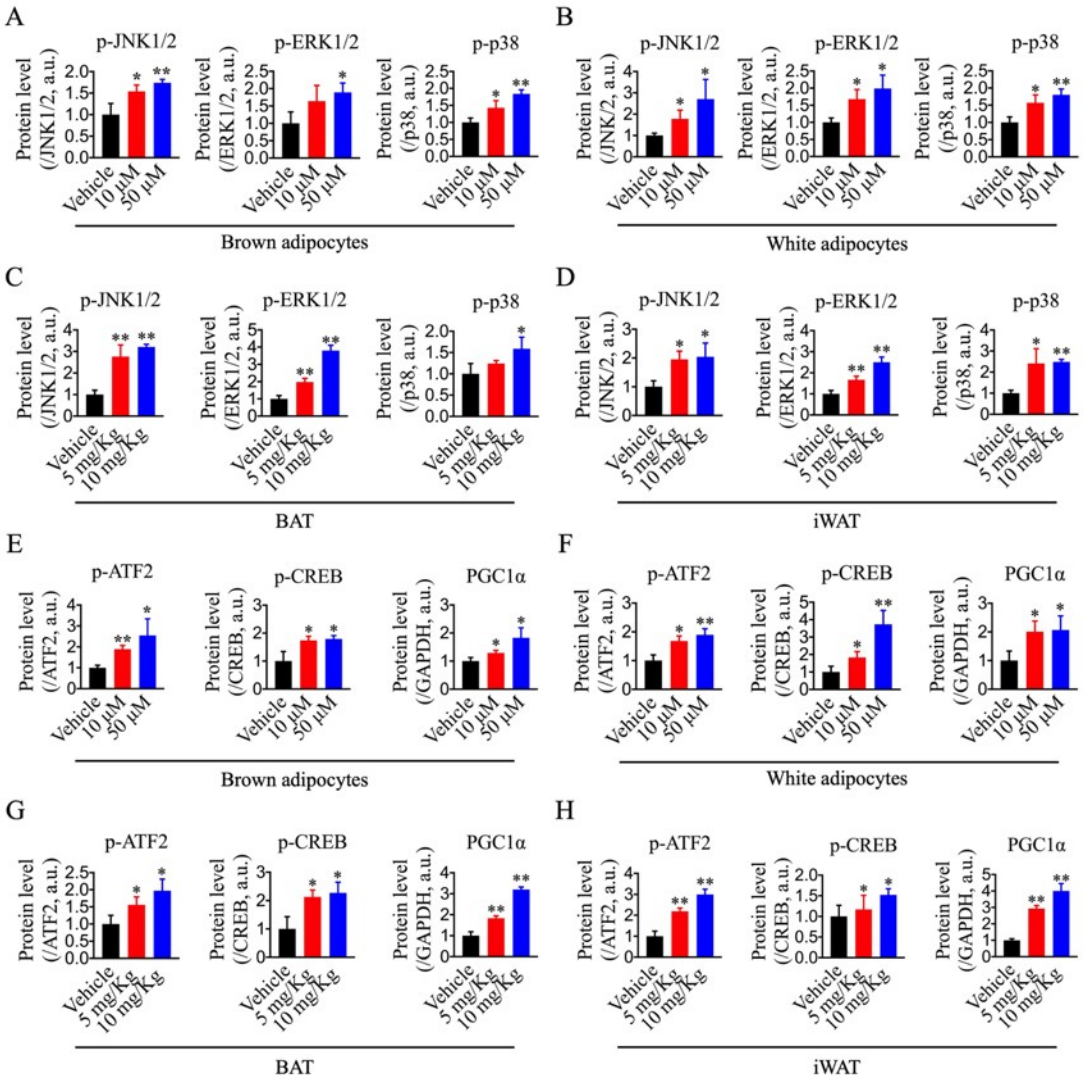

Supplemental Fig. S6 Quantization for the Western blot results of MAPK events
(A and B) Band intensity quantization of Western blot indicating the phosphorylation level changes of JNK, ERK1/2 and p38 in brown and white adipocytes treated with Miltin. (C and D) Densitometric analysis of JNK, ERK1/2 and p38 in BAT and iWAT from C57BL/6J mice fed a chow diet administrated with Miltin or vehicle for 2 weeks. (E and F) Band intensity quantization of Western blot indicating the phosphorylated and total protein levels of ATF2 and CREB as well as the PGC1α protein level in mature brown and white adipocytes treated as in panel A and B. (G and H) Densitometric analysis of ATF2, CREB and PGC1α in BAT and iWAT from C57BL/6J mice treated as in panel C and D. Data are presented as mean ± SD. $^{*}P < 0.05$ and $^{**}P < 0.01$ versus Vehicle, two-tailed unpaired Student's *t* tests.

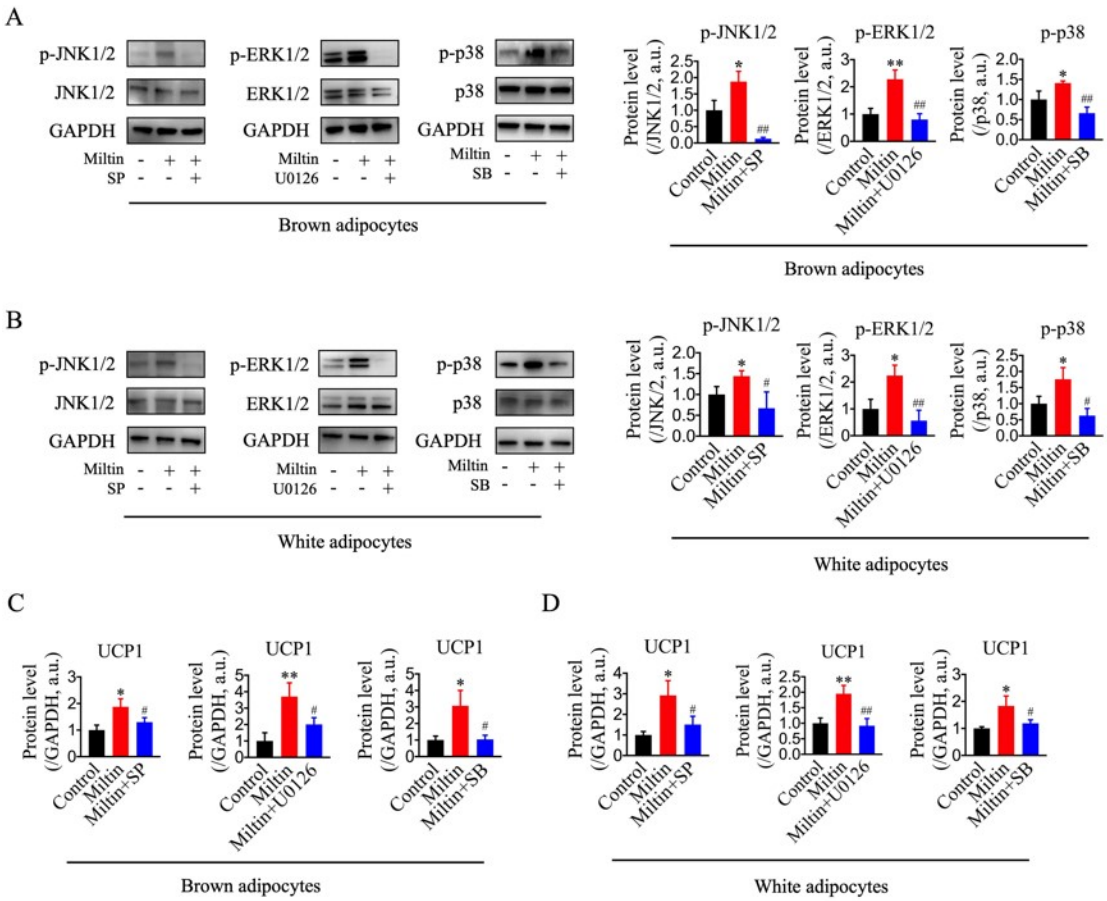

Supplemental Fig. S7 Miltin stimulates adipocyte thermogenesis through MAPK signaling pathway: JNK1/2, ERK1/2 and p38

(A and B) Immunoblots showing phosphorylated and total protein levels of JNK, ERK1/2 and p38 in Miltin-treated mature brown adipocytes and white adipocytes with or without corresponding inhibitors. (C and D) Band intensity quantization of Western blot indicating the protein levels of UCP1 in brown and white adipocytes treated with corresponding inhibitors. Data are presented as mean ± SD. $^{*}P < 0.05$ and $^{**}P < 0.01$ versus Control, $^{\#}P < 0.05$ and $^{\#\#}P < 0.01$ versus Miltin, two-tailed unpaired Student's *t*-tests.

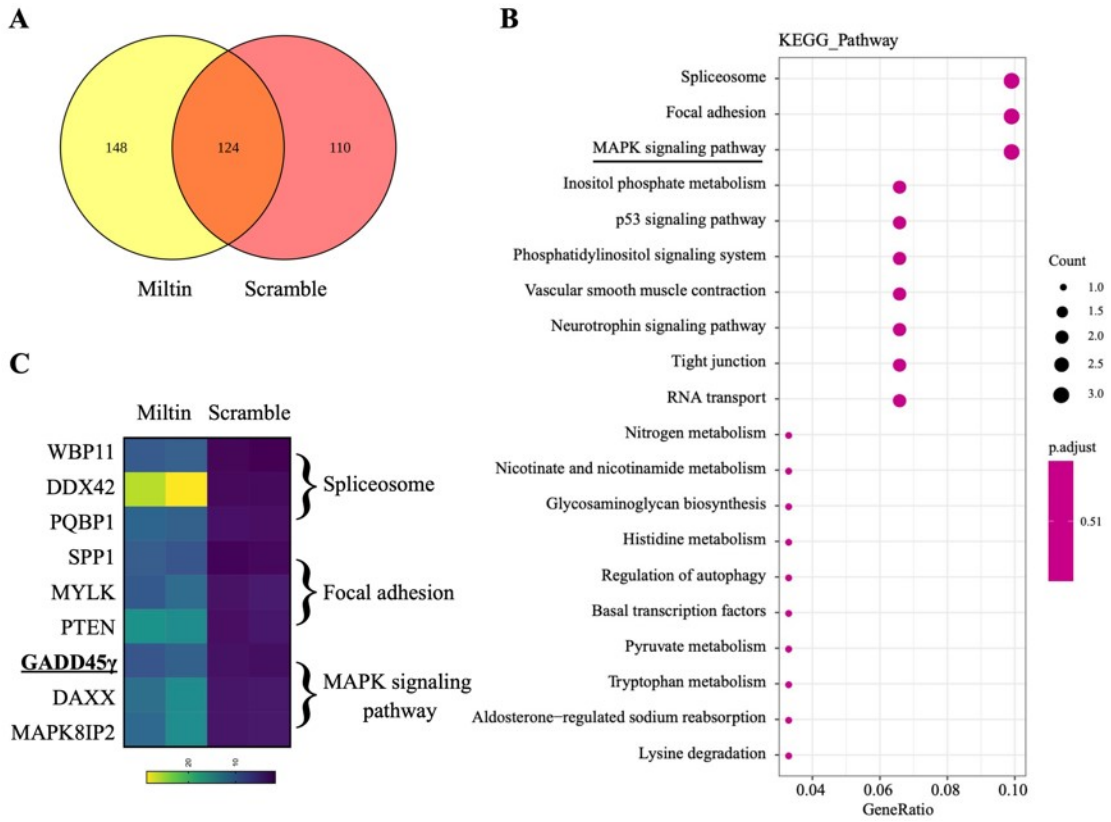

Supplemental Fig. S8 Screening of Miltin-binding proteins on the human proteome microarrays

(A) Cluster analysis to screen for candidate proteins potentially interacting with Miltin in brown adipocytes. Human proteome microarrays were incubated with biotinylated Miltin or scrambled control, followed by Cy5-labeled streptavidin for visualization. Yellow proteins bind to Miltin; red, proteins bind to scrambled peptide; orange, proteins bind to both. (B) KEGG analysis of pathways in Miltin-binding proteins. (C) Miltin-interacting proteins related to the top three pathways.

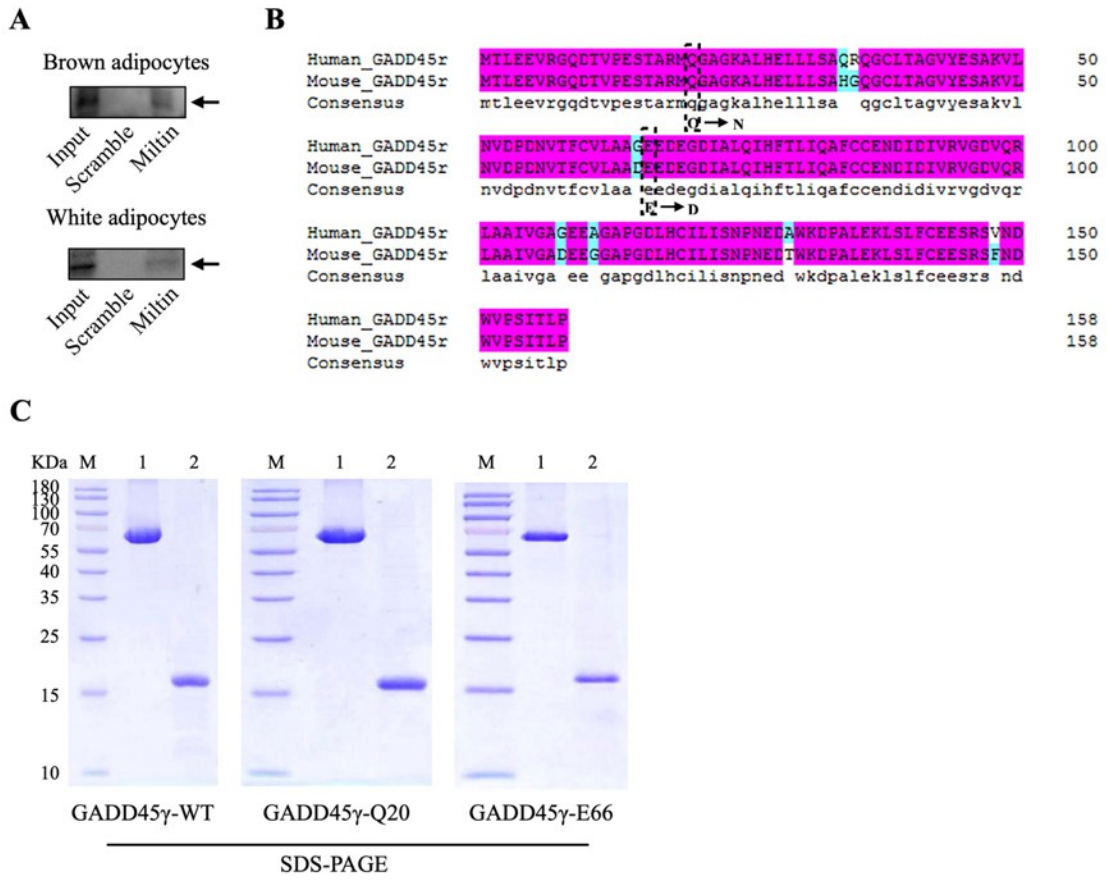

Supplemental Fig. S9 Purification of mutant recombinant GADD45γ proteins in *E. coli*

(A) Precipitation assays were performed to examine the interaction of Miltin and GADD45γ. Cell lysates (input) from brown and white adipocytes were used as positive controls. (B) Multiple alignments of the GADD45γ amino acid sequence between human and mouse species. (C) SDS-PAGE analysis of mutant recombinant GADD45γ proteins expressed in *E. coli*. Lane 1 indicates BAS control, while Lane 2 represents recombinant GADD45γ protein.

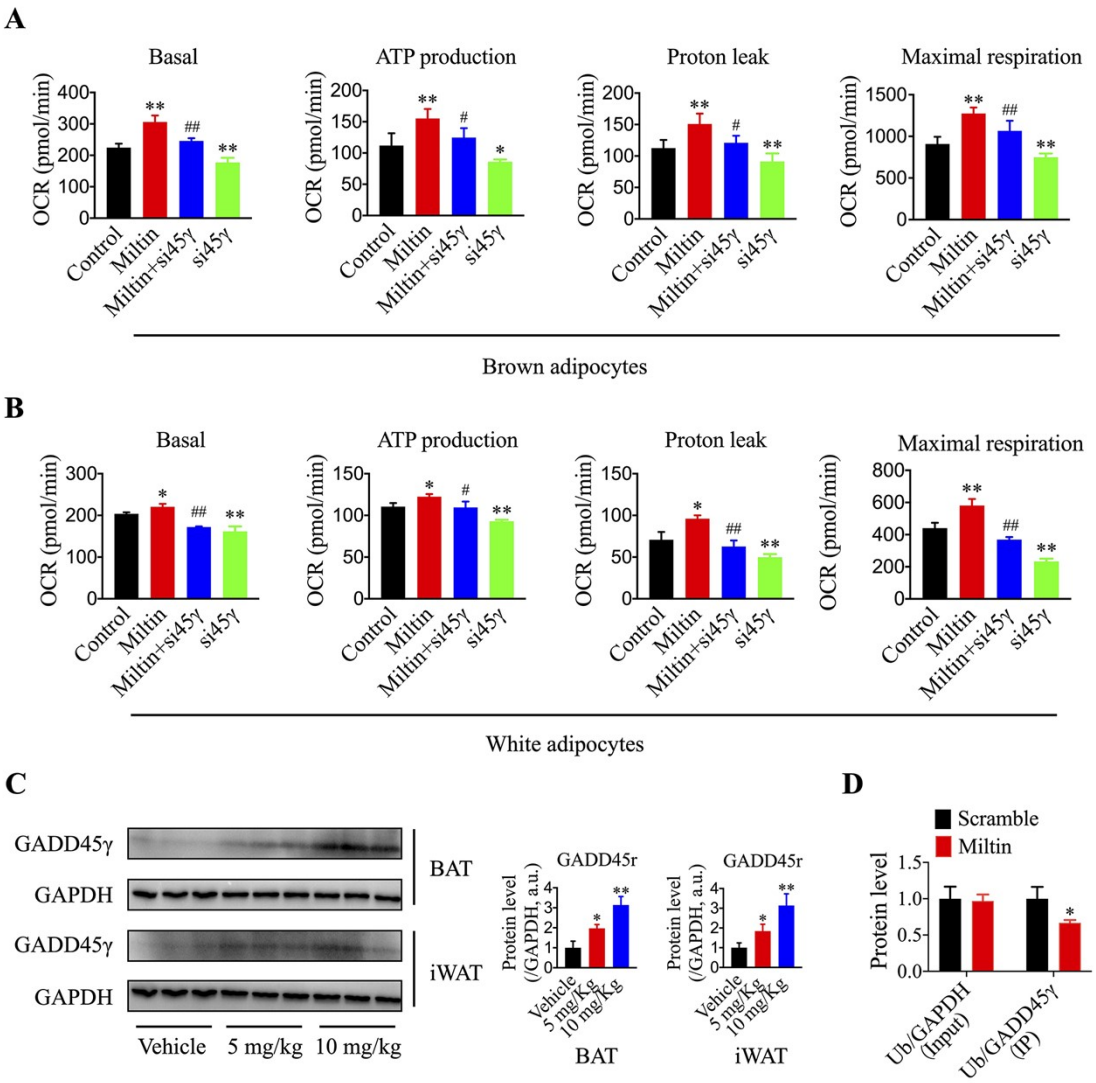

Supplemental Fig. S10 Miltin regulates adipocyte thermogenesis through GADD45γ

(A and B) Basal OCR, proton leak, ATP production and maximal respiration were quantified in brown and white adipocytes transfected with siRNAs targeting GADD45γ in the presence of Miltin or not. (C) Expression of UCP1 proteins in BAT and iWAT from mice with or without Miltin treatment daily for 2 weeks. (D) Ubiquitination levels of exogenous GADD45γ in 293T cells.

Supplemental table S1 Primers and siRNA sequences used in this study

Primer	Species	Sequence	Application
Ucp1	Human	F: CTGGAATAGCGGCGTGCTT R: AATAACACTGGACGTCGGGC	RT-PCR
	Mouse	F: AGGCTTCCAGTACCATTAGGT R: CTGAGTGAGGCAAAGCTGATTT	RT-PCR
Pparα	Human	F: GGCGAACGATTCGACTCAAG R: TCCAAAACGAATCGCGTTGT	RT-PCR
	Mouse	F: ACAAGGCCTCAGGGTACCA R: GCCGAAAGAAGCCCTTACAG	RT-PCR
Pgc1α	Human	F: ACCTGACACAACACGGACAG R: GTCTCCATCATCCCGCAGAT	RT-PCR
	Mouse	F: CCCTGCCATTGTTAAGACC R: TGCTGCTGTTCCTGTTTTC	RT-PCR
Dio2	Human	F: AGTGCAGAAGGAGGTGACAACAGT R: AAAGTCAAGAAGGTGGCATGTGGC	RT-PCR
	Mouse	F: GATGCTCCCAATTCCAGTGT R: TGAACCAAAGTTGACCACCA	RT-PCR
Cidea	Human	F: GATGCCCTCGTCATCGCTAC R: GCGTGTTGTCTCCCAAGGTC	RT-PCR
	Mouse	F: ATCACAACTGGCCTGGTTACG R: TACTACCCGGTGTCCATTTCT	RT-PCR
Ppia	Human	F: TTCATCTGCACTGCCAAGAC R: TCGAGTTGTCCACAGTCAGC	RT-PCR
	Mouse	F: GAGCTGTTTGCAGACAAAGTTC R: CCCTGGCACATGAATCCTGG R: GACAATGTCTGCTGGCTCAA	RT-PCR
Gadd45γ	Human	F: CGTCTACGAGTCAGCCAAAGTC R: CGATGTCGTTCTCGCAGCAGAA	RT-PCR
Gadd45γ	Human	F: GACAAUGUGACCUUCUGUTT R: CACAGAAGGUCACAUUGUCTT	siRNA